Thiolates *vs.* halides as π-donors: the redox-active alkyne complexes [M(SR)L(η-R′C≡CR′)L′] {M = Mo or W, L = CO or $P(OMe)_3$, L′ = η-C_5H_5 and Tp′}†

Christopher J. Adams, Angharad Baber, Supakorn Boonyuen, Neil G. Connelly,* Beatriz E. Diosdado, Anob Kantacha, A. Guy Orpen and Elena Patrón

Received 1st July 2009, Accepted 10th September 2009
First published as an Advance Article on the web 28th September 2009
DOI: 10.1039/b912986c

The cyclic voltammograms of the alkyne complexes [M(SR)L(η-R′C≡CR′)(η-C_5H_5)] (M = Mo or W, R = Me or Ph, R′ = Me or Ph) show two oxidation processes. Both are irreversible for the stereochemically rigid carbonyls (L = CO) but the first is reversible for the fluxional phosphites {L = $P(OMe)_3$}; the paramagnetic monocations [M(SPh){$P(OMe)_3$}(η-MeC≡CMe)(η-C_5H_5)]$^+$ were detected by ESR spectroscopy after *in situ* chemical one-electron oxidation. By contrast, the hydrotris(pyrazolyl)borate analogues [W(SR)(CO)(η-PhC≡CPh)Tp′] {R = Me or Ph, Tp′ = hydrotris(3,5-dimethylpyrazolyl)borate} are oxidised in two reversible steps to the corresponding mono- and dications; the redox pair [W(SPh)(CO)(η-PhC≡CPh)Tp′]^z (z = 0 and 1+) has been structurally characterised. A comparison of the redox potentials for the oxidation of [W(SR)(CO)(η-PhC≡CPh)Tp′] with those of the halide analogues [WX(CO)(η-PhC≡CPh)Tp′] suggests that the factors which give rise to the inverse halide order for the latter may not operate for the thiolates, which appear to be the better π-donors in all three redox states [WL(CO)(η-PhC≡CPh)Tp′]^z (L = halide or thiolate, z = 0, 1+ and 2+).

Introduction

During a study of the stepwise conversion of the (formally) d^5 alkyne complexes [$M(CO)_2$(η-RC≡CR)Tp′] {Tp′ = hydrotris(3,5-dimethylpyrazolyl)borate} to the d^2 cations [MX_2(η-RC≡CR)Tp′]$^+$ (M = Mo or W, X = F or Cl) *via* a sequence of one-electron transfer and substitution reactions,[1–3] we observed that the dependence of both the oxidation potential and ν(CO) of [MX(CO)(η-RC≡CR)Tp′] (in the order X = F < Cl < Br < I, *i.e.* an inverse halide order) was consistent with an ionic component to the M-X bond. The small size of fluorine, and therefore its proximity to the metal centre, leads to a higher energy HOMO and the lowest oxidation potential. In the d^3 monocations, [MX(CO)(η-RC≡CR)Tp′]$^+$, electronegativity effects become more important, leading to the order X = F < I < Br < Cl for both ν(CO) and the potential for the couple [MX(CO)(η-RC≡CR)Tp′]$^{2+}$/[MX(CO)(η-RC≡CR)Tp′]$^+$; high M-F π-donation is still facilitated by the short M-F distance.[2]

We have now investigated the redox chemistry of analogous complexes of thiolate ligands, also potential π-donors, where the structural effects observed on oxidation of the halides {a substantial shortening of the W–X bond on oxidation of [WX(CO)(η-RC≡CR)Tp′] (X = Cl and Br) to [WX(CO)(η-RC≡CR)Tp′]$^+$}[2] might be supplemented by redox-induced angular and orientational changes in the M-S-R unit, thereby providing more information on which to base quantitative bonding arguments. We therefore report (i) the synthesis, characterisation and electrochemistry of the d^4 complexes [W(SR)(CO)(η-PhC≡CPh)Tp′] (R = Me or Ph), (ii) a structural comparison of the redox pair [W(SPh)(CO)(η-PhC≡CPh)Tp′]^z (z = 0 and 1+) and (iii) the redox properties of a range of analogous cyclopentadienyl complexes, [M(SR)L(η-R′C≡CR′)(η-C_5H_5)] {M = Mo or W, L = CO or $P(OMe)_3$}, many of which are known[4–9] but have not been studied by electrochemical methods.

Results and discussion

Synthesis and characterisation of [M(SR)(CO)(η-R′C≡CR′)(η-C_5H_5)], [M(SR){$P(OMe)_3$}(η-R′C≡CR′)(η-C_5H_5)] and [W(SR)(CO)(η-PhC≡CPh)Tp′]

The carbonyls [M(SR)(CO)(η-R′C≡CR′)(η-C_5H_5)] (M = Mo, R′ = Me, R = Me **1** or Ph **2**; R′ = Ph, R = Me **3** or Ph **4**; M = W, R′ = Me, R = Me **5** or Ph **6**) were made by a modification of a published method,[9] *i.e.* by reacting the cationic bis(alkyne) complexes [M(CO)(η-R′C≡CR′)$_2$(η-C_5H_5)]X (M = Mo, R′ = Me, X = $[BF_4]^-$; M = Mo, R′ = Ph, X = $[BF_4]^-$; M = W, R′ = Me, X = $[PF_6]^-$) with NaSMe or with HSPh and NEt_3; the phosphite analogues [M(SR){$P(OMe)_3$}(η-R′C≡CR′)(η-C_5H_5)] (M = Mo, R′ = Me, R = Me **7** or Ph **8**; R′ = Ph, R = Me **9**; R′ = Ph, R = Ph **10** or M = W, R′ = Me, R = Ph **11**) were similarly prepared from the bis(phosphite) alkyne complexes [M{$P(OMe)_3$}$_2$(η-R′C≡CR′)(η-C_5H_5)]X (M = Mo, R′ = Me, X = $[BF_4]^-$; M = Mo, R′ = Ph, X = $[BF_4]^-$; M = W, R′ = Me, X = $[PF_6]^-$). The complexes [W(SR)(CO)(η-PhC≡CPh)Tp′] (R = Me **12** or Ph **13**) were

School of Chemistry, University of Bristol, Bristol, BS8 1TS, UK. E-mail: neil.connelly@bristol.ac.uk; Fax: +44 (0)117 929 0509; Tel: +44 (0)117 928 8162

† Electronic supplementary information (ESI) available: NMR spectroscopic data. CCDC reference numbers 738814–738822. For ESI and crystallographic data in CIF or other electronic format see DOI: 10.1039/b912986c

synthesised by treating $[W(CO)_2(\eta\text{-PhC}{\equiv}CPh)Tp'][BF_4]$ with NaSR (R = Me or Ph) in thf. (Complexes are identified in Scheme 1.)

Complex	M	R	L	R'	L'	*z*
1	Mo	Me	CO	Me	$\eta\text{-}C_5H_5$	0
2	Mo	Ph	CO	Me	$\eta\text{-}C_5H_5$	0
3	Mo	Me	CO	Ph	$\eta\text{-}C_5H_5$	0
4	Mo	Ph	CO	Ph	$\eta\text{-}C_5H_5$	0
5	W	Me	CO	Me	$\eta\text{-}C_5H_5$	0
6	W	Ph	CO	Me	$\eta\text{-}C_5H_5$	0
7	Mo	Me	$P(OMe)_3$	Me	$\eta\text{-}C_5H_5$	0
8	Mo	Ph	$P(OMe)_3$	Me	$\eta\text{-}C_5H_5$	0
9	Mo	Me	$P(OMe)_3$	Ph	$\eta\text{-}C_5H_5$	0
10	Mo	Ph	$P(OMe)_3$	Ph	$\eta\text{-}C_5H_5$	0
11	W	Ph	$P(OMe)_3$	Me	$\eta\text{-}C_5H_5$	0
12	W	Me	CO	Ph	Tp'	0
13	W	Ph	CO	Ph	Tp'	0
$\mathbf{12}^+$	W	Me	CO	Ph	Tp'	1+
$\mathbf{13}^+$	W	Ph	CO	Ph	Tp'	1+

Scheme 1 Complexes $[M(SR)L(\eta\text{-R'C}{\equiv}CR')L']^z$.

The cyclopentadienyl complexes **1–11** were isolated in good yield, after chromatography and subsequent crystallisation, but competing reactions appear to contribute to the low yields (less than 20%) of the Tp′ analogues **12** and **13**. An orange by-product, identified as $[W(SR)(CO)_2Tp']$ {R = Me, ν(CO) = 1838 and 1943 cm^{-1}; R = Ph, ν(CO) = 1821 and 1935 cm^{-1}},[10] was difficult to separate from $[W(SR)(CO)(\eta\text{-PhC}{\equiv}CPh)Tp']$ due to its similar solubility, and in the reaction between $[W(CO)_2(\eta\text{-PhC}{\equiv}CPh)Tp'][BF_4]$ and NaSPh the complex $[WF(CO)(\eta\text{-PhC}{\equiv}CPh)Tp']$ was also formed, as indicated by cyclic voltammetry and NMR and IR spectroscopy. It has been noted previously that heating $[W(CO)_2(\eta\text{-PhC}{\equiv}CMe)Tp'][BF_4]$ in thf gives $[W(FBF_3)(CO)(\eta\text{-PhC}{\equiv}CMe)Tp']$ or, if a nucleophile is present, $[WF(CO)(\eta\text{-PhC}{\equiv}CMe)Tp']$.[11]

Other attempts to improve the yields of **12** and **13** were unsuccessful. The reaction of $[W(CO)_2(\eta\text{-PhC}{\equiv}CPh)Tp'][BF_4]$ with PhSH and NEt_3 gave mainly $[WF(CO)(\eta\text{-PhC}{\equiv}CPh)Tp']$ with a very small amount of $[W(SPh)(CO)(\eta\text{-PhC}{\equiv}CPh)Tp']$. The complex $[WCl(CO)(\eta\text{-PhC}{\equiv}CPh)(\eta\text{-}C_5H_5)]$ reacts with TlSR (R = alkyl) to give $[W(CO)(SR)(\eta\text{-PhC}{\equiv}CPh)(\eta\text{-}C_5H_5)]$[8] but $[WCl(CO)(\eta\text{-PhC}{\equiv}CPh)Tp']$ did not react with TlSR (R = Me or Ph).

The relatively air-stable complexes **1–13** were characterised by elemental analysis, IR (Table 1) and NMR spectroscopy (see ESI†) and, for **1**, **3**, **4**, **7**, **8** and **11–13**, by X-ray crystallography. Their redox properties were studied by cyclic voltammetry (Table 1).

IR spectroscopy

Each of the IR spectra of $[M(SR)(CO)(\eta\text{-R'C}{\equiv}CR')(\eta\text{-}C_5H_5)]$ **1–6** and $[M(SR)(CO)(\eta\text{-PhC}{\equiv}CPh)Tp']$ (R = Me **12** or Ph **13**) in CH_2Cl_2 shows a single carbonyl band in the region 1898–1944 cm^{-1} but two bands with different intensities are resolved in *n*-hexane (Table 1). The two peaks are most likely due to isomers with different orientations of the SR group, as shown in Fig. 1 (*i.e.* the *syn* isomer with R orientated towards the $\eta\text{-}C_5H_5$ ring or Tp′ ligand and the *anti* isomer with R pointing toward the carbonyl and alkyne ligands) and as seen for $[Mo(SC_6F_5)(CO)(\eta\text{-}CF_3C{\equiv}CCF_3)(\eta\text{-}C_5H_5)]$.[5]

It is notable that the relative intensities, and therefore presumably the isomer distribution in solution, are very different for the

Table 1 Analytical data for alkyne thiolate complexes

			Analysis[a] (%)			ν(CO)[b]/cm^{-1}		E[c]/V	
Complex	Colour	Yield (%)	C	H	N	CH_2Cl_2	*n*-hexane	E_{ox}^1	E_{ox}^2
$[Mo(SMe)(CO)(\eta\text{-MeC}{\equiv}CMe)(\eta\text{-}C_5H_5)]$ **1**	Red	41	45.6 (45.5)	4.8 (4.9)	—	1916	1921w, 1934	0.54(I)	1.10(I)
$[Mo(SPh)(CO)(\eta\text{-MeC}{\equiv}CMe)(\eta\text{-}C_5H_5)]$ **2**	Red	81	54.7 (54.6)	4.6 (4.6)	—	1922	1893w, 1937	0.72(I)	1.17(I)[d]
$[Mo(SMe)(CO)(\eta\text{-PhC}{\equiv}CPh)(\eta\text{-}C_5H_5)]$ **3**	Green	65	61.0 (60.9)	3.9 (4.4)	—	1938	1939w, 1959	0.62(I)	1.21(I)
$[Mo(SPh)(CO)(\eta\text{-PhC}{\equiv}CPh)(\eta\text{-}C_5H_5)]$ **4**	Green	78	65.2 (65.5)	4.4 (4.2)	—	1944	1912w, 1957	0.77(I)	1.28(I)[e]
$[W(SMe)(CO)(\eta\text{-MeC}{\equiv}CMe)(\eta\text{-}C_5H_5)]$ **5**	Orange	51	35.3 (34.9)	3.8 (3.7)	—	1908	1909w, 1928	0.52(I)	0.93(I)
$[W(SPh)(CO)(\eta\text{-MeC}{\equiv}CMe)(\eta\text{-}C_5H_5)]$ **6**	Orange	57	45.2 (45.3)[f]	4.4 (4.1)	—	1916	1896w, 1930	0.63(I)	1.06(I)
$[Mo(SMe)\{P(OMe)_3\}(\eta\text{-MeC}{\equiv}CMe)(\eta\text{-}C_5H_5)]$ **7**	Blue	59	40.5 (40.4)	6.1 (6.0)	—	—	—	0.03[g]	0.77(I)
$[Mo(SPh)\{P(OMe)_3\}(\eta\text{-MeC}{\equiv}CMe)(\eta\text{-}C_5H_5)]$ **8**	Blue	72	48.1 (48.2)	5.9 (5.5)	—	—	—	0.18[g]	0.82(I)
$[Mo(SMe)\{P(OMe)_3\}(\eta\text{-PhC}{\equiv}CPh)(\eta\text{-}C_5H_5)]$ **9**	Green	36	54.1 (54.1)	5.2 (5.3)	—	—	—	0.12[g]	0.77(I)
$[Mo(SPh)\{P(OMe)_3\}(\eta\text{-PhC}{\equiv}CPh)(\eta\text{-}C_5H_5)]$ **10**	Green	76	58.2 (58.7)	4.7 (5.5)	—	—	—	0.24[g]	0.82(I)
$[W(SPh)\{P(OMe)_3\}(\eta\text{-MeC}{\equiv}CMe)(\eta\text{-}C_5H_5)]$ **11**	Pink	66	40.6 (40.3)	4.7 (4.7)	—	—	—	0.08[g]	0.63(I)
$[W(SMe)(CO)(\eta\text{-PhC}{\equiv}CPh)Tp']$ **12**	Green	18	50.8 (50.7)	4.7 (4.8)	11.4 (11.4)	1898	1906, 1918w	0.25[h]	1.08
$[W(SPh)(CO)(\eta\text{-PhC}{\equiv}CPh)Tp']$ **13**	Green	15	54.2 (54.3)	4.7 (4.7)	10.4 (10.6)	1910	1922, 1944w	0.32	1.06
$[W(SMe)(CO)(\eta\text{-PhC}{\equiv}CPh)Tp']^+$ $\mathbf{12}^{+i}$	Dark green	65	45.1 (45.3)	4.5 (4.3)	10.2 (10.2)	2046	—	0.25[h,j]	1.09
$[W(SPh)(CO)(\eta\text{-PhC}{\equiv}CPh)Tp']^+$ $\mathbf{13}^{+i}$	Dark green	58	48.5 (49.0)	3.8 (4.2)	9.5 (9.5)	2043	—	0.32[h,j]	1.05

[a] Calculated values in parentheses. [b] Strong absorptions unless stated otherwise, w = weak. [c] At a Pt electrode in CH_2Cl_2, with potentials relative to the saturated calomel electrode, calibrated *vs.* the $[Fe(\eta\text{-}C_5Me_5)_2]^+/[Fe(\eta\text{-}C_5Me_5)_2]$ couple (at –0.08 V) unless otherwise stated. For irreversible (I) processes, the peak potential, $(E_p)_{ox}$, is given at a scan rate of 200 mV s^{-1}. [d] Partially reversible reduction wave at –1.67 V. [e] Partially reversible reduction wave at –1.54 V. [f] Analysed as a 0.5 diethyl ether solvate. [g] Calibrated *vs.* the $[Fe(\eta\text{-}C_5H_5)_2]^+/[Fe(\eta\text{-}C_5H_5)_2]$ couple (at 0.47 V). [h] Calibrated *vs.* the $[Fe(\eta\text{-}C_5H_4COMe)(\eta\text{-}C_5H_5)]^+/[Fe(\eta\text{-}C_5H_4COMe)(\eta\text{-}C_5H_5)]$ couple (at 0.74 V). [i] Cations isolated as $[BF_4]^-$ salts. [j] One-electron reduction to the neutral complex.

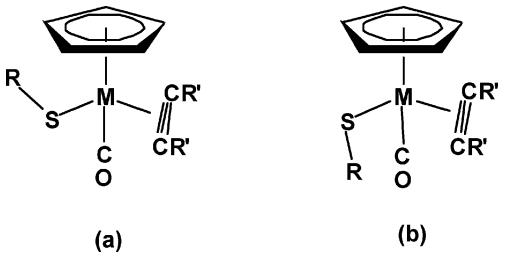

Fig. 1 The *syn* (a) and *anti* (b) isomers of [M(SR)(CO)(η-R′C≡CR′)(η-C_5H_5)].

η-C_5H_5 and Tp′ analogues. The higher energy band for the former is the more intense, *e.g.* **1** shows bands at 1921w and 1934s cm^{-1}, but this band is much the weaker in the latter, *e.g.* **12** shows bands at 1906s and 1918w cm^{-1}.

The carbonyl bands of [Mo(SR)(CO)(η-R′C≡CR′)(η-C_5H_5)] are lower in energy than those of the halide analogues [MoX(CO)(η-R′C≡CR′)(η-C_5H_5)] (X = Cl, Br or I)[12,13] by *ca.* 10 cm^{-1} (*e.g.* 1944 and 1954 cm^{-1} for [Mo(SPh)(CO)(η-PhC≡CPh)(η-C_5H_5)] **4** and [MoCl(CO)(η-PhC≡CPh)(η-C_5H_5)] respectively) suggesting the thiolate ligands to be the better donors. The lower energy of the carbonyl bands of [W(SMe)(CO)(η-PhC≡CPh)Tp′] **12** (1906s and 1918w cm^{-1}) relative to those of [W(SMe)(CO)(η-PhC≡CPh)(η-C_5H_5)] (1936w and 1944s cm^{-1})[8] implies that the Tp′ ligand is more electron donating than the cyclopentadienyl group. As Bergman and co-workers have noted, however, such comparisons of η-C_5H_5 and Tp′ ligands are not straightforward, their relative donating abilities depending on factors such as the group and oxidation state of the metal and the other ligands present in their complexes.[14]

NMR spectroscopy

NMR spectroscopic data for **1–13**, assigned by comparison with, for example, those for [Mo(SC_6H_4Ph-*o*)(CO)(η-MeC≡CMe)(η-C_5H_5)], [Mo(SePh){$P(OMe)_3$}(η-MeC≡CMe)(η-C_5H_5)][9] and [MX(CO)(η-RC≡CR)L] (M = Mo or W, X = halide, R = Me or Ph, L = η-C_5H_5[12,13] or Tp′[2,15]), are given in the ESI.†

Though the spectral assignment is mainly routine, several points are notable in relation to the fluxional processes possible for the thiolate alkyne complexes, *i.e.* rotation of the substituent R about the M-S or S-R bonds, alkyne rotation (about the metal-alkyne bond) and, in the diphenylacetylene complexes, rotation of the phenyl groups about the C-Ph bonds.

For both sets of carbonyl complexes, *i.e.* [M(SR)(CO)(η-R′C≡CR′)(η-C_5H_5)] **1–6** and [W(SR)(CO)(η-PhC≡CPh)Tp′] **12** and **13**, the alkyne is not rotating. Thus, at room temperature (i) two methyl singlets are observed for **1**, **2**, **5** and **6** in both the ^1H and ^{13}C spectra, *i.e.* the alkyne substituents are inequivalent, and (ii) two acetylenic carbons are observed for all but complex **4** (in the range expected for an alkyne acting as a four-electron donor, *i.e.* 175–250 ppm).[16] Non-rotating alkynes were also observed for [Mo(SC_6H_4Ph-*o*)(CO)(η-MeC≡CMe)(η-C_5H_5)][9] and [WR(CO)(η-HC≡CH)(η-C_5H_5)] (R = alkyl, *etc.*[17]).

By contrast, alkyne rotation does occur at room temperature for the phosphite derivatives **7–11**, with equivalent methyl carbons observed in both the ^1H and ^{13}C NMR spectra of the but-2-yne complexes **7**, **8** and **11** (and equivalent alkyne carbon atoms in the ^{13}C NMR spectrum of **8**).

At lower temperatures, however, alkyne rotation is stopped, illustrated by the ^1H NMR spectrum of [Mo(SPh){$P(OMe)_3$}(η-MeC≡CMe)(η-C_5H_5)] **8** (from 25 to –20 °C) in Fig. 2; the broad but-2-yne proton signal observed at room temperature (at 2.88 ppm) resolves into two singlets (at 2.67 and 3.01 ppm) at –20 °C. The barrier to rotation, Δ*G*, is 55.8(2) kJ mol^{-1} in CD_2Cl_2 {that for **7** is 60.3(3) kJ mol^{-1}}, in the same range as for related complexes such as [M(ER){$P(OMe)_3$}(η-MeC≡CMe)(η-C_5H_5)] (ER = SePh, SPh, $SC_6H_4NH_2$-*p*, SC_6H_4OMe-*p*, SC_6H_4Me-*p* and $SC_6H_4NO_2$-*p*), for which Δ*G* = 52–65 kJ mol^{-1} (in toluene).[9]

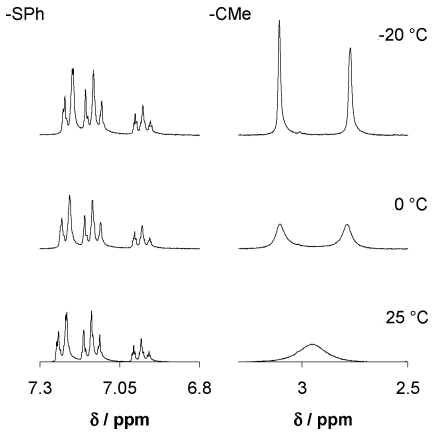

Fig. 2 The variable temperature ^1H NMR spectrum of [Mo(SPh){$P(OMe)_3$}(η-MeC≡CMe)(η-C_5H_5)] **8**.

The barrier to alkyne rotation in [MXY(η-alkyne)(η-C_5H_5)] depends on the difference in the π-acceptor abilities of X and Y; the greater the difference, the higher the barrier is to alkyne rotation.[18,19] The non-rotating alkyne (on the NMR spectroscopic timescale) in complexes **1–6** is consistent with the large difference in the π-acceptor abilities of CO and SR, the smaller difference between $P(OMe)_3$ and SR leading to alkyne rotation for complexes **7–11** (at room temperature). {However, alignment of the alkyne with the stronger π-acceptor, $P(OMe)_3$, is still favoured in the solid state. See below for X-ray crystallographic studies on **7**, **8** and **11**, and as found for [M($SC_6H_4NO_2$-*p*){$P(OMe)_3$}(η-MeC≡CMe)(η-C_5H_5)].[9]}

Although *syn* and *anti* isomers of **2–6**, **12** and **13** were detected by IR spectroscopy in the carbonyl region, they were not distinguishable in the room temperature ^1H NMR spectra; the interconversion of the two isomers, which would occur by rotation about the M-S bond (or inversion at sulfur), is presumably fast on the NMR spectroscopic time scale. For species such as [Mo(SCF_3)(CO)(η-CF_3C≡CCF_3)(η-C_5H_5)][4] and [Mo(SMe)(CO)(η-MeC≡CMe)(η-C_5H_5)] **1**[9] isomer interconversion was not observed on the IR spectroscopic time scale.

A quantitative ^{19}F NMR spectroscopic study[7] of [W(SC_6F_5)-(CO)(η-CF_3C≡CCF_3)(η-C_5H_5)] showed three fluxional processes, with rotation of the aryl ring about the S–C_6F_5 bond occurring at lower energy than rotation about the W–S bond which was lower in energy than alkyne rotation. Phenyl rotation about the S–C_6H_5 bond is observed for all of the phenylthiolate complexes **2**, **4**, **6**, **8**,

10 and **11**, each showing equivalent pairs of *o*- and *m*-protons (in the case of **8**, even at –20 °C).

Although the two phenyl groups of the alkyne of the cyclopentadienyl carbonyl complexes [Mo(SR)(CO)(η-PhC≡CPh)(η-C_5H_5)] (M = Mo, R = Me **3** or Ph **4**) are inequivalent, each rotates about its C-Ph bond (the pairs of *o*- and *m*-positions in each aryl ring are equivalent). In the $P(OMe)_3$ derivatives **9** and **10** the equivalent (by alkyne rotation) phenyl groups also rotate about the C-Ph bonds.

A variable temperature NMR spectroscopic study of the Tp′ complexes **12** and **13** verifies that the *syn* and *anti* isomers interconvert. The six Tp′ methyl singlets observed in the ^{1}H NMR spectrum of [W(SPh)(CO)(η-PhC≡CPh)Tp′] **13** at 20 °C are labelled *a*–*f* in Fig. 3. As the temperature is lowered, each of the peaks *a*, *c* and *f* splits into two, giving rise to six singlets at 0.55, 1.63, 2.29, 2.32, 2.42, 2.96 ppm in the ratio 2 : 1 : 1 : 1 : 2 : 2. By contrast, the singlets *b*, *d* and *e* are largely unaffected by temperature. The most likely explanation is that at low temperature two isomers of [W(SPh)(CO)(η-PhC≡CPh)Tp′] can be observed in a 2 : 1 ratio, but only the three methyl groups in the 3-positions of the pyrazole rings give different resonances for the two isomers.

The singlet at 0.55 ppm may correspond to a 3-methyl group of the isomer that has the phenyl ring of the thiolate pointing toward the Tp′ ligand [*i.e.* the *syn* isomer, Fig. 1(a)]; it is slightly upfield for a methyl group of a Tp′ ligand due to the local magnetic field created by the phenyl ring.[20] This would then suggest that the major isomer is *syn*-[W(SPh)(CO)(η-PhC≡CPh)Tp′] as found in the solid state (see below). One would then assign the IR carbonyl band at lower wave number to this isomer.

The peaks *g*, *h* and *i* (Fig. 3) in the room temperature spectrum are assigned to the protons at the 4-positions of the pyrazolyl rings of the Tp′ ligand. At low temperature, five sharp peaks are observed; three, at 5.66, 5.83 and 5.86 ppm, correspond to the minor isomer but only two singlets, at 5.72 and 5.92 ppm, are observed for the major isomer. However, a broad peak at 5.49 ppm may also be assigned to the major isomer.

At –90 °C the observation of several multiplets and many broad peaks in the phenyl region of the ^{1}H NMR spectrum of [W(SPh)(CO)(η-PhC≡CPh)Tp′] makes the assignment of signals impossible. In the variable temperature ^{1}H NMR spectra of [W(SMe)(CO)(η-PhC≡CPh)Tp′] **12** only the multiplet between 6.31–6.40 ppm at 20 °C changes, disappearing at low temperature. Unfortunately, splitting of this multiplet is not resolved at –90 °C.

The ^{13}C-{^{1}H} NMR spectra of [W(SR)(CO)(η-PhC≡CPh)Tp′] (R = Me **12** or Ph **13**) show five (**12**) or six (**13**) peaks for the carbon atoms of the Tp′ methyl groups and three each for the carbons in the 3-, 4- and 5-positions of the pyrazolyl rings. Thus, the three pyrazolyl rings are inequivalent as also shown by the ^{1}H NMR spectrum.

The carbon atom of the thiolate methyl group of [W(SMe)(CO)(η-PhC≡CPh)Tp′] **12** is slightly deshielded at 8.02 ppm. The three phenyl groups in [W(SPh)(CO)(η-PhC≡CPh)Tp′] **13** are mostly observed in the same region (123–138 ppm), making the assignment of the peaks complicated. However, a comparison between the spectra of **12** and **13** allows the peaks at 123.63, 127.34, 131.72 and 151.77 ppm to be assigned to the thiolate phenyl group of the latter. The assignment of signals to the carbon atoms of the S-Ph group has been made on the basis of the published ^{13}C-{^{1}H} NMR spectrum of [Mo(SPh){$P(OMe)_3$}(η-MeC≡CMe)(η-C_5H_5)] **9**.[9] Moreover, the observation of only four peaks suggests that the thiolate phenyl ring rotates about the C–S bond at room temperature.

For **12** and **13**, the phenyl substituents of the alkyne ligand give only eight resonances (the two most deshielded can be assigned to the *ipso* carbons) showing these phenyl groups to rotate at room temperature.

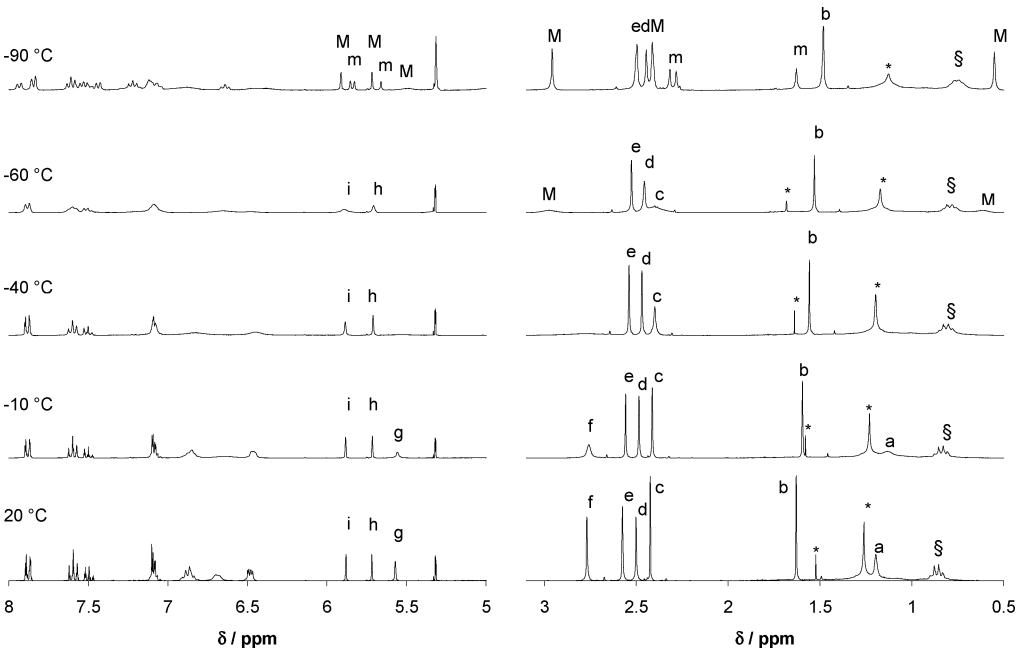

Fig. 3 Variable temperature ^{1}H NMR spectra of [W(SPh)(CO)(η-PhC≡CPh)Tp′] **13**. * Impurity; § *n*-hexane; M major isomer; m minor isomer.

Electrochemical studies

The electrochemical behaviour of the three series of complexes [Mo(SR)(CO)(η-R′C≡CR′)(η-C_5H_5)] **1–6**, [M(SR){P(OMe)$_3$}(η-R′C≡CR′)(η-C_5H_5)] **7–11** and [W(SR)(CO)(η-PhC≡CPh)Tp′] **12** and **13** is significantly different, reflecting the various factors that contribute to the accessibility of the one-electron oxidation product and its reactivity. In each case, cyclic voltammetry was carried out at a Pt disc electrode in CH_2Cl_2.

The CVs of **1–6** are generally similar; that of [W(SPh)(CO)(η-MeC≡CMe)(η-C_5H_5)] **6** is shown in Fig. 4(a) as a representative example. Each complex shows two irreversible oxidation waves, the first between 0.52 and 0.77 V and the second in the range 0.93 and 1.28 V (Table 1). In this case, the monocations [Mo(SR)(CO)(η-R′C≡CR′)(η-C_5H_5)]$^+$ (M = Mo or W, R = Me or Ph, R′ = Me or Ph) **1**$^+$–**6**$^+$ are unstable on the timescale of cyclic voltammetry, and the product formed after their (unspecified) reaction gives a second redox-active species which is also unstable on oxidation.

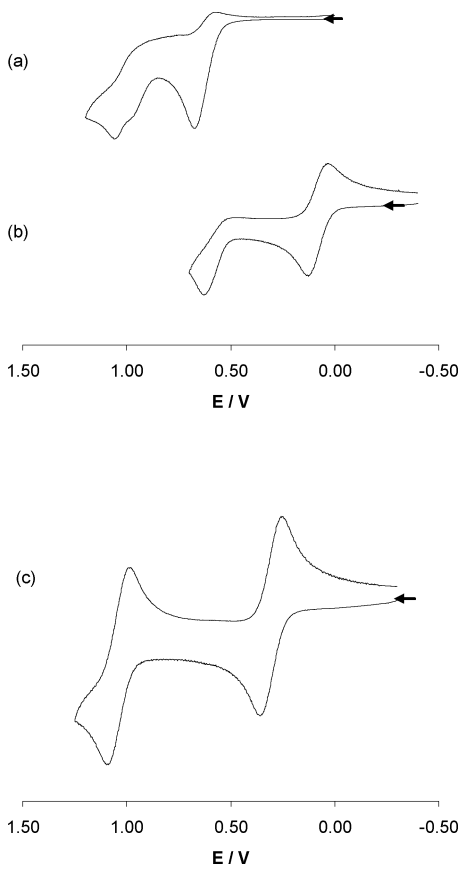

Fig. 4 CVs of (a) [W(SPh)(CO)(η-MeC≡CMe)(η-C_5H_5)] **6**, (b) [W(SPh){P(OMe)$_3$}(η-MeC≡CMe)(η-C_5H_5)] **11** and (c) [W(SPh)(CO)-(η-PhC≡CPh)Tp′] **13**.

On replacing CO by P(OMe)$_3$ the CVs of [M(SR){P(OMe)$_3$}(η-R′C≡CR′)(η-C_5H_5)] **7–11** {shown in Fig. 4(b) for **11**} are similar to each other, but different from those of **1–6**; the first oxidation process is shifted to a more negative potential, by *ca*. 0.5 V, and also becomes reversible. The paramagnetic monocations [M(SR){P(OMe)$_3$}(η-R′C≡CR′)(η-C_5H_5)]$^+$ **7**$^+$–**11**$^+$ should therefore be both more chemically accessible and more kinetically stable than [M(SR)(CO)(η-R′C≡CR′)(η-C_5H_5)]$^+$ **1**$^+$–**6**$^+$. The second oxidation wave of **7–11** is, however, irreversible, showing that the dications [M(SR){P(OMe)$_3$}(η-R′C≡CR′)(η-C_5H_5)]$^{2+}$ **7**$^{2+}$–**11**$^{2+}$ undergo further reaction.

On replacing η-C_5H_5 in [W(SR)(CO)(η-PhC≡CPh)(η-C_5H_5)] by Tp′, [W(SR)(CO)(η-PhC≡CPh)Tp′] (R = Me **12** or Ph **13**) undergoes two reversible oxidations, shown for **13** in Fig. 4(c), implying both the monocations, **12**$^+$ and **13**$^+$, and the dications, **12**$^{2+}$ and **13**$^{2+}$, are stable (at least on the CV timescale).

The redox behaviour of the thiolate complexes **12** and **13** is similar to that of the halide analogues [WX(CO)(η-PhC≡CPh)Tp′] (X = F, Cl, Br or I)[2] for which the first oxidation is reversible. However, the second oxidation process differs in two ways. First, it is reversible for the thiolate complexes but irreversible for the halide complexes. Second, the cationic halide complexes [WX(CO)(η-PhC≡CPh)Tp′]$^+$ are oxidised to the dications at potentials *ca.* 500 mV more positive than are the analogous thiolates.

The stability of [W(SR)(CO)(η-PhC≡CPh)Tp′]$^+$ relative to [W(SR)(CO)(η-PhC≡CPh)(η-C_5H_5)]$^+$ is probably a result of the steric protection provided by the Tp′ ligand. However, the stabilisation of the d^2 dication [W(SR)(CO)(η-PhC≡CPh)Tp′]$^{2+}$ relative to [WX(CO)(η-PhC≡CPh)Tp′]$^{2+}$ (X = halide)[2] is possibly a result of more effective π-donation by the thiolate (see below).

Chemical oxidation

The low potential for, and reversibility of, the oxidation of [M(SR){P(OMe)$_3$}(η-R′C≡CR′)(η-C_5H_5)] **7–11** and [W(SR)-(CO)(η-PhC≡CPh)Tp′] (R = Me **12** or Ph **13**) suggested that the paramagnetic monocations **7**$^+$–**13**$^+$ should be readily formed from the neutral complexes on treatment with one equivalent of a mild one-electron oxidant.

Attempts to isolate the cations [M(SPh){P(OMe)$_3$}(η-MeC≡CMe)(η-C_5H_5)]$^+$ (M = Mo or W) were unsuccessful although their ESR spectra have been recorded after *in situ* oxidation of **7–11** using [Fe(η-C_5H_5)$_2$]$^+$ (see below). However, the salts [W(SR)(CO)(η-PhC≡CPh)Tp′][BF_4] (R = Me **12**$^+$[BF_4]$^-$ or Ph **13**$^+$[BF_4]$^-$) were synthesised as dark green solids in good yield by treating [W(SR)(CO)(η-PhC≡CPh)Tp′] (R = Me **12** or Ph **13**) with [Fe(η-C_5H_4COMe)(η-C_5H_5)][BF_4] in CH_2Cl_2. The two complexes were characterised by elemental analysis, cyclic voltammetry (which showed one reversible oxidation wave and one reversible reduction wave at potentials identical to those of the two oxidations of the neutral complexes, Table 1) and IR and ESR spectroscopy.

The cation [W(SPh)(CO)(η-PhC≡CPh)Tp′]$^+$ was also synthesised as the [PF_6]$^-$ salt [W(SPh)(CO)(η-PhC≡CPh)Tp′][PF_6] **13**$^+$[PF_6]$^-$ by using [Fe(η-C_5H_5)$_2$][PF_6]. Although, the cyclic voltammogram of the product showed contamination by residual [Fe(η-C_5H_5)$_2$]$^+$, and a pure sample (by elemental analysis) could not be obtained, slow crystallisation from CH_2Cl_2–*n*-hexane gave a few green crystals of the salt which were analysed by X-ray crystallography (see below).

Each of the IR spectra of [W(SR)(CO)(η-PhC≡CPh)Tp′]$^+$ (R = Me **12**$^+$ or Ph **13**$^+$) in CH_2Cl_2 (Table 1) shows a single carbonyl peak (2046 and 2043 cm^{-1} for R = Me and Ph respectively), 148 and 133 cm^{-1} higher respectively than those of the neutral complexes, *i.e.* there is a much less back donation from the metal to the carbonyl group in the cations.

Table 2 ESR spectroscopic data for $[M(SR)L(\eta\text{-}R'C{\equiv}CR')L']^+$

Complex	Isotropic parameters[a]				Anisotropic parameters[a]						
	$<g>$	T/K	$<A^M>$	$<A^P>$	T/K	g_1	g_2	g_3	g_{ave}	A^M	A^P
$[Mo(SPh)\{P(OMe)_3\}(\eta\text{-}MeC{\equiv}CMe)(\eta\text{-}C_5H_5)]^+$ **8**$^+$	2.0033	183	21.9	7.8	109	2.030	2.012	1.983	2.009	[b]	11, 22, 14
$[W(SPh)\{P(OMe)_3\}(\eta\text{-}MeC{\equiv}CMe)(\eta\text{-}C_5H_5)]^+$ **11**$^+$	1.9888	240	32.0	13.0	110	2.043	2.001	1.942	1.996	[b]	26, 29, 23
$[W(SMe)(CO)(\eta\text{-}MeC{\equiv}CMe)Tp']^+$ **12**$^+$	1.9698	290	43.0	—	120	2.023	1.985	1.899	1.969	28, 56, 40	—
$[W(SPh)(CO)(\eta\text{-}MeC{\equiv}CMe)Tp']^+$ **13**$^+$	1.9608	290	43.0	—	120	2.017	1.964	1.895	1.958	27, 60, 42	—

[a] Recorded in CH_2Cl_2-thf (1 : 2); hyperfine coupling constants in 10^{-4} cm^{-1}. [b] Not determined.

ESR spectroscopy

The ESR spectra of $[W(SR)(CO)(\eta\text{-}PhC{\equiv}CPh)Tp'][BF_4]$ (R = Me **12**$^+[BF_4]^-$ or Ph **13**$^+[BF_4]^-$) were recorded in CH_2Cl_2-thf (1 : 2) between 120 and 290 K. As noted above, the cations $[Mo(SPh)\{P(OMe)_3\}(\eta\text{-}MeC{\equiv}CMe)(\eta\text{-}C_5H_5)]^+$ **8**$^+$ and $[W(SPh)\{P(OMe)_3\}(\eta\text{-}MeC{\equiv}CMe)(\eta\text{-}C_5H_5)]^+$ **11**$^+$ could not be isolated. However, they were generated at low temperature, *in situ*, by freezing (77 K) the neutral complexes **8** and **11** in a mixture of CH_2Cl_2-thf (1 : 2) in an ESR tube, adding solid $[Fe(\eta\text{-}C_5H_5)_2][PF_6]$, transferring the tube to the ESR spectrometer at *ca.* 130 K, and then increasing the temperature to 160 K until oxidation occurred. Re-cooling the sample allowed the spectra to be recorded in the range 110–130 K; warming the sample to 280 K gave the isotropic spectrum.

The isotropic ESR spectra of **8**$^+$ and **11**$^+$-**13**$^+$ all consist of a single signal showing satellites due to hyperfine coupling to the spin-active isotopes of the metal ($^{95/97}$Mo, I = 5/2, 24.5%; ^{183}W, 14.8% I = 1/2), and in the case of the trimethylphosphite complexes **8**$^+$ and **11**$^+$ to the ^{31}P (I =1/2) nucleus as well (Table 2). The isotropic spectrum of **8**$^+$ is shown in Fig. 5 as an example.

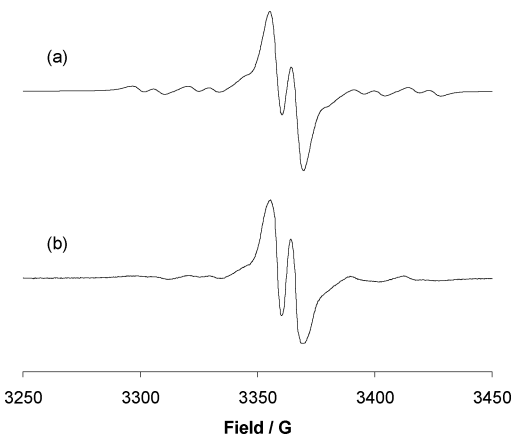

Fig. 5 The isotropic ESR spectrum of $[Mo(SPh)\{P(OMe)_3\}(\eta\text{-}MeC{\equiv}CMe)(\eta\text{-}C_5H_5)]^+$ **8**$^+$ in CH_2Cl_2-thf (1 : 2); (a) simulated spectrum and (b) experimental spectrum at 183 K.

The anisotropic spectra of **12**$^+$ (Fig. 6) and **13**$^+$ consist of three separated *g*-features, each showing tungsten satellites, and are readily simulated. The anisotropic spectra of **8**$^+$ and **11**$^+$ are less readily interpreted, though appearing straightforward. Each apparently contains a doublet on the high-field *g* component, and several components to lower field. Attempts to model these lower-field signals have not produced very satisfactory results; parameters for the best models obtained by assuming that all

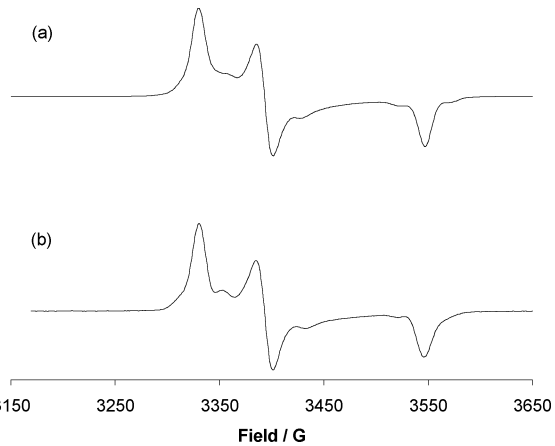

Fig. 6 The anisotropic ESR spectrum of $[W(SMe)(CO)(\eta\text{-}PhC{\equiv}CPh)Tp']^+$ **12**$^+$ in CH_2Cl_2-thf (1 : 2); (a) simulated spectrum and (b) experimental spectrum at 120 K.

three *g* components are doublets are given in Table 2, and the experimental and simulated spectra of **11**$^+$ are shown in Fig. 7. However, there are obvious features in the spectra unaccounted for by the models, and $<g>$ differs from g_{ave} calculated from the simulation for these complexes. Our best interpretation of these results is that the observed spectra are superpositions of those arising from two different species in the frozen glass; perhaps the cation freezes into both *syn* and *anti* conformations which give distinct spectra.

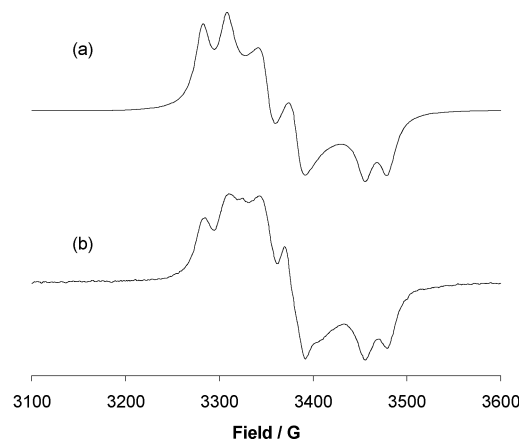

Fig. 7 The anisotropic ESR spectrum of $[W(SPh)\{P(OMe)_3\}(\eta\text{-}MeC{\equiv}CMe)(\eta\text{-}C_5H_5)]^+$ **11**$^+$ in CH_2Cl_2-thf (1 : 2); (a) simulated spectrum and (b) experimental spectrum at 110 K.

The spectra of $\mathbf{12}^+$ and $\mathbf{13}^+$ may be compared with those of the halide complexes $[WX(CO)(\eta\text{-MeC}\equiv\text{CMe})Tp']^+$ (X = F, Cl, Br or I). In that series, g_{iso} increased on descending the halogen group whilst $A_{iso}{}^W$ increased; the values for $[WBr(CO)(\eta\text{-MeC}\equiv\text{CMe})Tp']^+$ ($g_{iso} = 1.957$ G, $A_{iso}{}^W = 49.6\times10^{-4}$ cm^{-1}) are most similar to those of $\mathbf{13}^+$ ($g_{iso} = 1.961$ G, $A_{iso}{}^W = 43.0\times10^{-4}$ cm^{-1}). Using our previous methodology, from the g and A_W values it is possible to estimate the contribution of the tungsten d_{yz} orbital to the SOMO, $(c_{yz})^2$. The g and A_W values for $\mathbf{12}^+$ and $\mathbf{13}^+$ (Table 2) give $(c_{yz})^2 = 0.53$ and 0.50 respectively, *i.e.* the SOMO is 50% based on the tungsten d_{yz} orbital, similar to the value of 0.56 for $[WF(CO)(\eta\text{-MeC}\equiv\text{CMe})Tp']^+$.

The X-ray structures of 1, 3, 4, 7, 8, 11–13 and 13$^+$

Single crystal X-ray diffraction studies on nine examples (**1**, **3**, **4**, **7**, **8**, **11–13** and $\mathbf{13}^+$) of complexes with the general formula $[M(SR)L(\eta\text{-R}'\text{C}\equiv\text{CR}')L']^{\mp}$ {M = Mo or W, R = Me or Ph, L = CO or $P(OMe)_3$, R′ = Me or Ph, z = 0 or 1+} have allowed comparisons to be made of the effects of R (**3** *vs.* **4**), R′ (**1** *vs.* **3** and **12** *vs.* **13**), L (**1** *vs.* **7**), M (**8** *vs.* **11**) and z (**13** *vs.* $\mathbf{13}^+$) on structure and bonding. The molecular structures of **1**, **4**, **11**, **12**, **13** (one molecule of the two, **13A** and **13B**, in the asymmetric unit) and $\mathbf{13}^+$ are shown in Fig. 8–12 respectively with important bond lengths and angles listed in Tables 3 and 4.

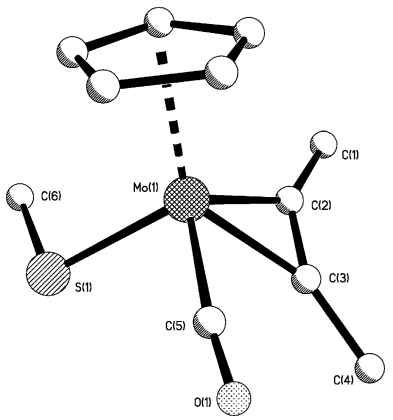

Fig. 8 Molecular structure of $[Mo(SMe)(CO)(\eta\text{-MeC}\equiv\text{CMe})(\eta\text{-}C_5H_5)]$ **1** (hydrogen atoms have been omitted for clarity).

The $\eta\text{-}C_5H_5$ complexes may be described as having the three-legged piano stool geometry, with an *S*-bonded thiolate, a trimethylphosphite or carbonyl ligand, and a π-bound alkyne forming the legs and the cyclopentadienyl ring the seat. Alternatively, all of the complexes can be regarded as octahedral with the $\eta\text{-}C_5H_5$ and Tp′ ligands occupying three *facial* sites.

In all of the cyclopentadienyl complexes, and in $[W(SPh)(CO)(\eta\text{-PhC}\equiv\text{CPh})Tp']$ **13**, the substituent on sulfur points towards the $\eta\text{-}C_5H_5$ or Tp′ ligand, *i.e.* all have the *syn* structure shown in Fig. 1(a). Uniquely, in **12** the methyl group points away from the Tp′ ligand and towards the CO ligand, *i.e.* it is *anti*-$[W(SMe)(CO)(\eta\text{-PhC}\equiv\text{CPh})Tp']$ (Fig. 11). For all of the carbonyl complexes, both *syn* and *anti* isomers are detectable by IR spectroscopy in *n*-hexane. The observation of only one isomer in each of the X-ray studies suggests that it crystallises selectively; it is not necessarily the dominant isomer in solution.

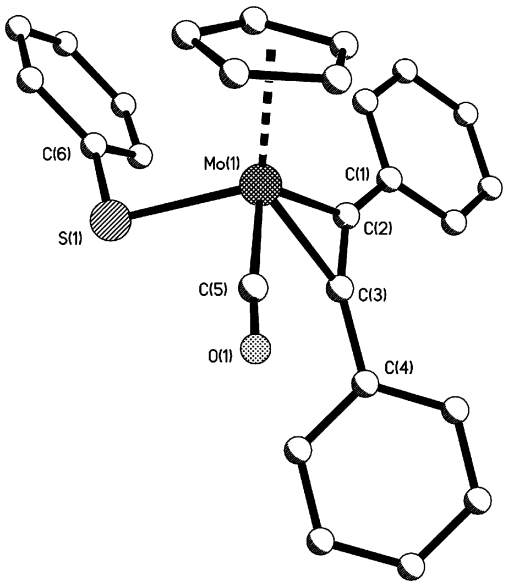

Fig. 9 Molecular structure of $[Mo(SPh)(CO)(\eta\text{-PhC}\equiv\text{CPh})(\eta\text{-}C_5H_5)]$ **4** (hydrogen atoms have been omitted for clarity).

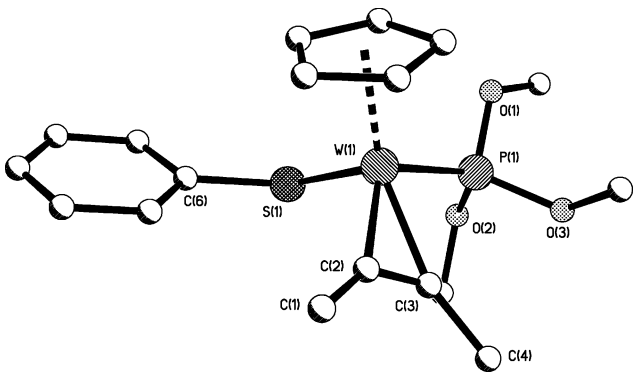

Fig. 10 Molecular structure of $[W(SPh)\{P(OMe)_3\}(\eta\text{-MeC}\equiv\text{CMe})(\eta\text{-}C_5H_5)]$ **11** (hydrogen atoms have been omitted for clarity).

The metal-alkyne bond lengths of the nine complexes vary between 2.011(3) and 2.104(7) Å. That these distances are generally rather longer than the upper end of the range reported for four-electron alkyne complexes (2.02 to 2.04 Å) was attributed[16] {for $[Mo(SC_6H_4NO_2\text{-}p)\{P(OMe)_3\}(\eta\text{-MeC}\equiv\text{CMe})(\eta\text{-}C_5H_5)]$, with Mo–$C_{alkyne}$ distances of 2.020(3) and 2.057(3) Å [9]} to a competition between thiolate and alkyne π-donation. However, the C≡C alkyne bond lengths are in the expected range (1.27–1.33 Å).[16]

In all cases there is significant asymmetry in the M(alkyne) unit; the contact carbon closer to the carbonyl ligand or phosphorus atom of the phosphite is further from the metal atom, *e.g.* 2.089(2) *vs.* 2.032(2) Å for **1**. Such asymmetry was also observed in $[Mo(SC_6F_5)(CO)(\eta\text{-}CF_3\text{C}\equiv\text{CCF}_3)(\eta\text{-}C_5H_5)]$,[5] $[Mo(SC_6H_4SPh\text{-}o)(CO)(\eta\text{-MeC}\equiv\text{CMe})(\eta\text{-}C_5H_5)]$ and $[Mo(SC_6H_4NO_2\text{-}p)\{P(OMe)_3\}(\eta\text{-MeC}\equiv\text{CMe})(\eta\text{-}C_5H_5)]$.[9]

Also in all cases, the alkyne is more closely aligned with the better π-acceptor ligand, *i.e.* CO in **1**, **3**, **4**, **12**, **13** and $\mathbf{13}^+$ and $P(OMe)_3$ in **7**, **8** and **11**, as expected[4,5,18,19,21] and as found

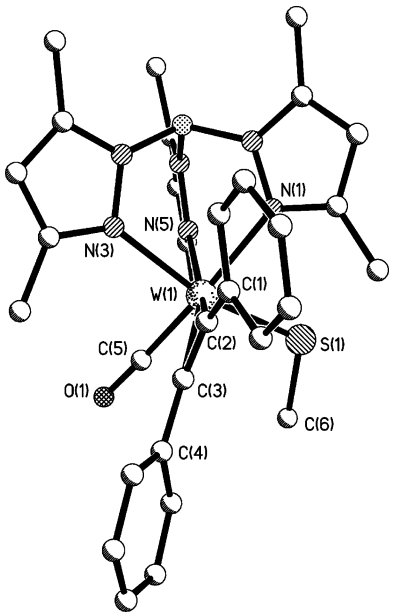

Fig. 11 Molecular structure of [W(SMe)(CO)(η-PhC≡CPh)Tp′] **12** (hydrogen atoms have been omitted for clarity).

in [Mo(SC_6F_5)(CO)(η-$CF_3C{\equiv}CCF_3$)(η-C_5H_5)],[5] [Mo(SC_6H_4SPh-*o*)(CO)(η-MeC≡CMe)(η-C_5H_5)], [Mo($SC_6H_4NO_2$-*p*){$P(OMe)_3$}-(η-MeC≡CMe)(η-C_5H_5)][9] and the halide complexes [MX(CO)(η-RC≡CR)Tp′].[2]

The complexes [M(SPh){$P(OMe)_3$}(η-MeC≡CMe)(η-C_5H_5)] (M = Mo **8** and W **11**) are essentially isostructural (Tables 3 and 5), *i.e.* there is no metal effect in this pair at least. For all nine complexes, the M-S distances, in the range 2.346(1)–2.396(3) Å, are between single and double bond values (Mo-SAryl, 2.40; Mo-SAlkyl, 2.40; W-SAryl, 2.42; W-SAlkyl, 2.47 Å[22]), suggesting π-donation from sulfur to metal as found in [W(SR)$(CO)_2$Tp′].[10]

Other pairwise comparisons support this suggestion. Thus, although the differences are small (as in all of the pairs described here), in analogous MeC≡CMe and PhC≡CPh complexes (**1** and **3**, and **12** and **13**) but-2-yne (the better net donor) leads to a smaller M-S-R angle and (for **12** and **13**) a longer W–S bond, consistent with less thiolate π-donation. Likewise, in the PhC≡CPh complexes [Mo(SR)(CO)(η-PhC≡CPh)(η-C_5H_5)] (R = Me **3** or Ph **4**), the SMe complex has the shorter Mo–S distance and larger Mo–S-Me angle. Finally, a comparison of [Mo(SMe)L(η-MeC≡CMe)(η-C_5H_5)] {L = CO **1** or $P(OMe)_3$ **7**} shows the shorter Mo–S distance for the carbonyl.

Potentially of most interest, however, is a comparison of the redox pair [W(SPh)(CO)(η-PhC≡CPh)Tp′]^z ($z = 0$ **13** and 1+ **13**$^+$) though this is somewhat limited by the relatively poor quality of the structure of **13** and the presence of two independent (and structurally distinct) molecules, **13A** and **13B**, in the unit cell.

The most obvious change is the lengthening of the W–C(O) bond on oxidation, from 1.990(9) Å in **13A** {1.959(11) Å in **13B**} to 2.064(7) Å in **13**$^+$, consistent with less back donation to the π*(CO) orbital in the latter and the large increase observed in ν(CO) (see above). Other differences are marginal but perhaps worth mentioning. First, the W–C_{alk} distances do not change significantly on oxidation, contrasting with the lengthening of *ca.* 0.02 Å observed on one-electron oxidation of [WX(CO)(η-MeC≡CMe)Tp′] (X = Cl or Br) where the HOMO is weakly π-bonding with respect to the W–C_{alk} bond.[2] The C(2)-C(3) alkyne distances and the C_{ipso}-C_{alk}–C_{alk} angles, C(1)-C(2)-C(3) and C(2)-C(3)-C(4), are also largely invariant, as is the W–S bond length. However, the narrowing of the W(1)-S(1)-C(6) angle in [W(SPh)(CO)(η-PhC≡CPh)Tp′] {116.7(3)° in **13A** and 116.5(3)° in **13B**} by 2°, to 118.8(2)° in [W(SPh)(CO)(η-PhC≡CPh)Tp′]$^+$ **13**$^+$, might suggest increased π-donation in the cation.

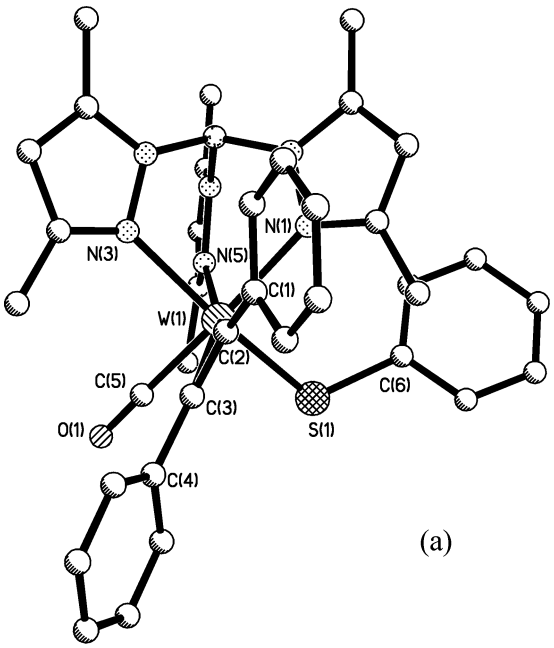

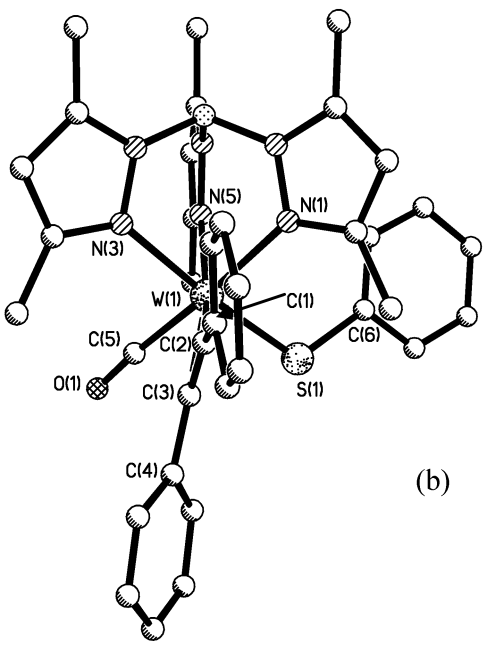

Fig. 12 Structures of (a) one independent molecule of [W(SPh)(CO)-(η-PhC≡CPh)Tp′] **13** and (b) [W(SPh)(CO)(η-PhC≡CPh)Tp′]$^+$ **13**$^+$ (hydrogen atoms have been omitted for clarity).

Table 3 Important bond lengths (Å) and angles (°) for [M(SR)(CO)(η-RC≡CR)(η-C_5H_5)] and [Mo(SR){P(OMe)$_3$}(η-RC≡CR)(η-C_5H_5)]

	1	**3**	**4**	**7**	**8**	**11**
C(2)-C(3)	1.289(3)	1.296(4)	1.299(2)	1.294(4)	1.293(6)	1.302(8)
M(1)-C(2)	2.032(2)	2.028(3)	2.044(2)	2.011(3)	2.012(4)	2.016(6)
M(1)-C(3)	2.089(2)	2.072(3)	2.075(2)	2.069(3)	2.074(4)	2.062(5)
M(1)-S(1)	2.354(1)	2.346(1)	2.370(1)	2.375(1)	2.379(1)	2.381(2)
M(1)-P(1)	—	—	—	2.330(1)	2.347(1)	2.356(2)
C(5)-O(1)	1.157(3)	1.140(3)	1.146(2)	—	—	—
M(1)-C(5)	1.934(2)	1.966(2)	1.946(2)	—	—	—
M(1)-C(C_5H_5)$_{ave}$	2.365(4)	2.365(1)	2.348(7)	2.356(1)	2.344(2)	2.351(7)
C(1)-C(2)-C(3)	143.2(2)	142.9(3)	143.4(2)	141.7(3)	141.7(4)	140.2(6)
C(2)-C(3)-C(4)	143.8(2)	139.9(3)	144.4(2)	137.8(3)	135.7(4)	134.8(6)
C(2)-M(1)-C(3)	36.4(1)	36.9(1)	36.8(1)	37.0(1)	36.8(2)	37.2(2)
S(1)-M(1)-C(2)	107.5(1)	107.9(1)	109.0(1)	106.4(1)	108.5(1)	107.3(2)
S(1)-M(1)-C(3)	105.7(1)	110.4(1)	104.8(1)	107.3(1)	108.0(1)	107.0(2)
S(1)-M(1)-P(1)	—	—	—	93.3(1)	84.2(1)	85.2(1)
P(1)-M(1)-C(2)	—	—	—	114.3(1)	118.3(1)	119.2(2)
P(1)-M(1)-C(3)	—	—	—	77.5(1)	81.4(1)	82.0(2)
M(1)-S(1)-C(6)	106.7(1)	108.3(1)	105.3(1)	105.3(1)	111.6(1)	111.9(2)
C(5)-M(1)-C(2)	108.5(1)	112.3(1)	112.0(1)	—	—	—
C(5)-M(1)-C(3)	72.1(1)	76.1(1)	75.5(1)	—	—	—
C(5)-M(1)-S(1)	90.9(1)	82.4(1)	89.5(1)	—	—	—
M(1)-C(5)-O(1)	173.2(2)	178.9(3)	173.5(2)	—	—	—
β_{CO}[a]	4.2(2)	11.4(2)	8.0(1)	—	—	—
β_P[b]	—	—	—	4.3(2)	2.2(3)	1.1(4)

[a] β_{CO} = dihedral angle formed by the M(1)-C(5) and C(2)-C(3) bonds. [b] β_P = dihedral angle formed by the C(2)-C(3) and M(1)-P(1) bonds.

Table 4 Important bond lengths (Å) and angles (°) for [W(SR)(CO)(η-PhC≡CPh)Tp′]^z

	12	**13A**	**13B**	**13$^+$**
C(2)–C(3)	1.299(9)	1.273(12)	1.289(12)	1.292(8)
W(1)–C(2)	2.069(6)	2.051(10)	2.044(9)	2.055(6)
W(1)–C(3)	2.104(7)	2.068(10)	2.077(10)	2.084(5)
W(1)–S(1)	2.374(1)	2.395(3)	2.396(2)	2.388(2)
C(6)–S(1)	1.821(4)	1.800(9)	1.784(10)	1.766(6)
W(1)–C(5)	1.934(5)	1.990(9)	1.959(11)	2.064(7)
C(5)–O(1)	1.174(5)	1.112(10)	1.143(11)	1.141(7)
W(1)–N(1)[a]	2.238(4)	2.248(7)	2.237(7)	2.169(5)
W(1)–N(3)[a]	2.242(3)	2.218(8)	2.216(7)	2.151(5)
W(1)–N(5)	2.247(6)	2.261(8)	2.227(8)	2.212(4)
C(1)–C(2)–C(3)	144.8(5)	141.9(10)	139.9(10)	145.4(6)
C(2)–C(3)–C(4)	139.2(6)	140.2(10)	143.8(10)	143.5(6)
N(1)–W(1)–N(3)	86.3(1)	86.9(3)	85.1(3)	87.5(2)
N(1)–W(1)–N(5)	81.2(2)	84.1(3)	84.8(3)	84.7(2)
N(3)–W(1)–N(5)	77.1(2)	76.1(3)	77.6(3)	79.2(2)
C(2)–W(1)–C(3)	36.3(3)	36.0(3)	36.4(3)	36.4(2)
S(1)–W(1)–C(2)	106.4(2)	109.3(3)	106.9(2)	105.5(2)
S(1)–W(1)–C(3)	98.6(2)	97.1(3)	96.6(3)	86.1(2)
S(1)–W(1)–C(5)	95.7(2)	87.2(3)	86.8(3)	87.0(2)
C(5)–W(1)–C(2)	107.9(2)	107.3(4)	106.5(4)	105.5(2)
C(5)–W(1)–C(3)	73.6(2)	73.1(4)	71.1(4)	74.0(2)
W(1)–S(1)–C(6)	114.0(2)	116.7(3)	116.5(3)	118.8(2)
W(1)–C(5)–O(1)	177.6(4)	178.9(10)	179.0(10)	174.6(5)
β_{CO}[b]	19.8(4)	18.2(7)	13.9(7)	30.9(4)
β_S[c]	82.0(4)	75.0(6)	77.8(6)	60.3(4)
$\Delta\beta$[d]	62.2	56.8	63.9	30.4

[a] N(1) is *trans* to the carbonyl group; N(3) is *trans* to sulfur. [b] β_{CO} = dihedral angle formed by the W(1)-C(5) and C(2)-C(3) bonds. [c] β_S = dihedral angle formed by the W(1)–S(1) and C(2)-C(3) bonds. [d] $\Delta\beta = |\beta_S - \beta_{CO}|$.

Finally, the alkyne aligns less with the W–C(O) bond (by *ca.* 13–17°) on oxidation, as also observed in the redox pairs [WX(CO)(η-MeC≡CMe)Tp′]^z ($z = 0$ or 1+; X = Cl or Br).[2]

The π-donor properties of halides *vs.* thiolates

As noted above, both [WX(CO)(η-PhC≡CPh)Tp′] and [W(SR)(CO)(η-PhC≡CPh)Tp′] undergo two one-electron oxidations, the associated redox potentials being more negative for the thiolate than the halide complexes in both steps, *i.e.* the thiolates are the best net donors in both the neutral and monocationic complexes. However, for the first step the redox potentials follow the order E°′ = SMe < SPh ≈ F < Cl < Br < I whereas that order is E°′ = SMe ≈ SPh << F < I < Br < Cl for the second step.

We have noted previously[2] that there is an inverse halide order for the halide complexes which appears to switch off at the second oxidation step. Interestingly, the plot of E°′ *vs.* ν(CO) {Fig. 13(a)} for the second oxidation of both [WX(CO)(η-PhC≡CPh)Tp′] and [W(SR)(CO)(η-PhC≡CPh)Tp′], *i.e.* to their dications, is linear ($R^2 = 0.98$) supporting 'normal' behaviour for the halides in the monocations. However, the plot for the first step {Fig. 13(b)} is not, and the thiolates appear to be considerably better net donors than the halides. In other words, the effect that results in an inverse halide order for the first one-electron oxidation of the halide complexes [WX(CO)(η-PhC≡CPh)Tp′] (X = F, Cl, Br or I) does not necessarily result in a more electron-rich metal centre. Given that the inverse halide order may relate more to the ionic nature of X, that component is likely to be least for the more polarisable thiolate ligands. In other words, the inverse halide order which is switched off for the halides after one-electron oxidation does not occur at all for the thiolates which are simply very good π-donors. That ability is carried through to the second oxidation step, thus leading to much lower (relative) redox potentials and the stabilisation of the higher [formally W(IV)] oxidation state in the dications.

The shifts in carbonyl stretching frequency, Δ(CO), seen on oxidation of the halide complexes [WX(CO)(η-PhC≡CPh)Tp′]

Table 5 Crystal and refinement data for [Mo(SMe)(CO)(η-MeC≡CMe)(η-C_5H_5)] **1**, [Mo(SMe)(CO)(η-PhC≡CPh)(η-C_5H_5)] **3**, [Mo(SPh)(CO)(η-PhC≡CPh)(η-C_5H_5)] **4**, [Mo(SMe){P(OMe)$_3$}(η-MeC≡CMe)(η-C_5H_5)] **7**, [Mo(SPh){P(OMe)$_3$}(η-MeC≡CMe)(η-C_5H_5)] **8**, [W(SPh){P(OMe)$_3$}(η-MeC≡CMe)(η-C_5H_5)] **11**, [W(SMe)(CO)(η-PhC≡CPh)Tp′] **12**, [W(SPh)(CO)(η-PhC≡CPh)Tp′] **13**, [W(SPh)(CO)(η-PhC≡CPh)Tp′][PF_6] **13**$^+$[PF_6]$^-$

Compound	**1**	**3**	**4**	**7**	**8**	**11**	**12**	**13**	**13**$^+$[PF_6]$^-$
Formula	$C_{11}H_{14}MoOS$	$C_{21}H_{18}MoOS$	$C_{26}H_{30}MoOS$	$C_{13}H_{23}O_3PSMo$	$C_{18}H_{25}O_3PSMo$	$C_{18}H_{25}O_3SWP$	$C_{31}H_{35}BN_6OSW$	$C_{36}H_{37}BN_6OSW$	$C_{36}H_{37}BF_6N_6OPSW$
M	290.22	414.36	476.42	386.28	448.35	536.26	734.37	796.44	941.41
Crystal system	Monoclinic	Monoclinic	Monoclinic	Monoclinic	Orthorhombic	Orthorhombic	Orthorhombic	Monoclinic	Triclinic
Space group (no.)	$P2_1/c$ (14)	$P2_1$ (4)	$P2_1/c$ (14)	$P2_1/c$ (14)	$P2_12_12_1$ (19)	$P2_12_12_1$ (19)	$Pca2_1$ (29)	$P2_1/c$ (14)	$P\bar{1}$ (2)
a/Å	13.771(3)	10.424(3)	11.382(6)	8.933(1)	7.417(2)	7.398(1)	16.178(1)	24.431(5)	10.644(2)
b/Å	12.510(3)	7.808(2)	10.380(4)	13.728 (2)	12.505(3)	12.589(1)	11.542(1)	10.460(2)	11.582(1)
c/Å	6.951(1)	10.812(2)	17.901(5)	13.322 (2)	20.942(4)	21.201(2)	16.357(1)	39.276(6)	15.604(2)
α (°)	90	90	90	90	90	90	90	90	81.89(1)
β (°)	101.33(3)	93.77 (2)	103.72(3)	90.82 (1)	90	90	90	127.62(1)	81.18(1)
γ (°)	90	90	90	90	90	90	90	90	83.88(1)
T/K	100(2)	100(2)	100(2)	100(2)	173(2)	173(2)	173(2)	173(2)	173(2)
U/Å^3	1174.1(4)	878.1(4)	2054.5(4)	1633.5(4)	1942.4(7)	1974.5(4)	3054.3(4)	7950(2)	1874.7(4)
Z	4	2	4	4	4	4	4	8	2
μ/mm^{-1}	1.260	0.869	0.755	1.029	1.533	6.049	3.885	2.991	3.248
Absolute structure parameter		–0.01(3)			–0.03(5)	0.015(10)	–0.002(14)		
Reflections collected	13225	10261	23164	18396	13737	12981	13635	79506	20055
Independent reflections (R_{int})	2694 (0.0547)	4003 (0.0373)	4708 (0.0468)	3751 (0.0520)	4455 (0.0649)	4450 (0.0466)	4734 (0.0360)	18227 (0.1636)	8508 (0.0628)
Final *R* indices [$I > 2\sigma(I)$]: *R*1, *wR*2	0.0254, 0.0561	0.0249, 0.0548	0.0231, 0.0603	0.0273, 0.0649	0.0407, 0.0780	0.0285, 0.0575	0.0251, 0.0436	0.0639, 0.1301	0.0447, 0.0800

Fig. 13 Plots of $E^{\circ\prime}$ *vs.* ν(CO) for the second (a) and first (b) one-electron oxidations of [WX(CO)(η-RC≡CR)Tp′] (X = F, Cl, Br, I, SMe or SPh).

{Δ(CO) for F (180 cm^{-1}) > Cl (174 cm^{-1}) > Br (169 cm^{-1}) > I (158 cm^{-1}} are somewhat less for the thiolates {*i.e.* Δ(CO) for SMe and SPh are 148 and 133 cm^{-1}, respectively}.[2] The decreasing sensitivity of the carbonyl ligand in [WX(CO)(η-PhC≡CPh)Tp′] to the effect of oxidation in the order shown suggested[2] that the contribution of the carbonyl ligand to the SOMO of [WX(CO)(η-PhC≡CPh)Tp′]$^+$ is greatest for X = F and least for X = I. The thiolates therefore lead to an even smaller contribution, also reflected in the ESR spectroscopic results where both the *g* and A^W values for **12**$^+$ and **13**$^+$ are much closer to those of the Br and I complexes than to those of Cl or F.

Conclusions

The molybdenum and tungsten thiolate complexes [M(SR)(CO)(η-R′C≡CR′)(η-C_5H_5)] (R = Me or Ph, R′ = Me or Ph) and [W(SR)(CO)(η-PhC≡CPh)Tp′] (R = Me or Ph) exist as *syn* and *anti* isomers, detectable by IR spectroscopy in *n*-hexane. The *syn* isomer is predominant for the cyclopentadienyl complexes (as found in the crystallographically characterised complexes [M(SR)(CO)(η-R′C≡CR′)(η-C_5H_5)] (M = Mo, R = Me, R′ = Me or Ph; M = W, R = Me, R′ = Ph) whereas the *anti* isomer dominates in solution for the hydrotris(pyrazolyl)borate analogues (though the structure of *syn*-[W(SPh)(CO)(η-PhC≡CPh)Tp′] has been determined in the solid state).

Variable temperature NMR spectroscopic studies show the carbonyls of [M(SR)(CO)(η-R′C≡CR′)(η-C_5H_5)] to be stereochemically rigid, whereas alkyne rotation is observed for the phosphite analogues [M(SR){P(OMe)$_3$}(η-R′C≡CR′)(η-C_5H_5)].

In the solid state, the alkyne is aligned approximately parallel to the M-CO or M-$P(OMe)_3$ bond, *i.e.* with the better π-acceptor ligand.

One-electron oxidation of $[M(SR)(CO)(\eta\text{-}R'C{\equiv}CR')(\eta\text{-}C_5H_5)]$ gives the unstable monocation $[M(SR)(CO)(\eta\text{-}R'C{\equiv}CR')(\eta\text{-}C_5H_5)]^+$ but replacing CO by $P(OMe)_3$ causes the first oxidation potential to decrease by *ca.* 0.5 V, and the oxidation wave to become reversible. The paramagnetic monocations $[M(SR)\{P(OMe)_3\}(\eta\text{-}R'C{\equiv}CR')(\eta\text{-}C_5H_5)]^+$ were detected by ESR spectroscopy.

Replacing $\eta\text{-}C_5H_5$ in $[W(SR)(CO)(\eta\text{-}PhC{\equiv}CPh)(\eta\text{-}C_5H_5)]$ by Tp′, giving $[W(SR)(CO)(\eta\text{-}PhC{\equiv}CPh)Tp']$ (R = Me or Ph) results in the observation of two reversible one-electron oxidation waves; treatment with one equivalent of $[Fe(\eta\text{-}C_5H_4COMe)(\eta\text{-}C_5H_5)][BF_4]$ gave the isolable salts $[W(SR)(CO)(\eta\text{-}PhC{\equiv}CPh)Tp'][BF_4]$. Structural characterisation of the redox pair $[W(SPh)(CO)(\eta\text{-}PhC{\equiv}CPh)Tp']^z$ (z = 0 and 1+) and of $[W(SMe)(CO)(\eta\text{-}PhC{\equiv}CPh)Tp']$ showed the alkyne more closely aligned with the C–O bond in the neutral complexes, and partial loss of this alignment in the case of the cation.

A comparison of the redox properties of $[WX(CO)(\eta\text{-}PhC{\equiv}CPh)Tp']$ (X = F, Cl, Br or I) with those of $[W(SR)(CO)(\eta\text{-}PhC{\equiv}CPh)Tp']$ suggest that the effects which cause an inverse halide order for the first oxidation of the former do not apply to the thiolates. Moreover, the thiolates act as the best π-donors throughout the redox series $[WX(CO)(\eta\text{-}PhC{\equiv}CPh)Tp']^z$ (z = 0, 1+ and 2+).

Experimental

The preparation, purification and reactions of the complexes described were carried out under an atmosphere of dry nitrogen using dried and deoxygenated solvents purified either by distillation or by using Anhydrous Engineering double alumina or alumina-copper catalyst drying columns. Reactions were monitored by IR spectroscopy where necessary. Unless stated otherwise, complexes were purified using a mixture of two solvents. The impure solid was dissolved in the more polar solvent, the resulting solution was filtered and then treated with the second solvent, and the mixture reduced in volume *in vacuo* to induce precipitation. Unless otherwise stated, complexes are stable under nitrogen and dissolve in polar solvents such as CH_2Cl_2 to give moderately air-stable solutions. The compounds $[M(CO)(\eta\text{-}RC{\equiv}CR)_2(\eta\text{-}C_5H_5)][BF_4]$ (M = Mo, R = Me or Ph;[23] M = W, R = Me[24]), $[Mo\{P(OMe)_3\}_2(\eta\text{-}MeC{\equiv}CMe)(\eta\text{-}C_5H_5)][BF_4]$ (R = Me or Ph),[23] $[W(CO)_2(\eta\text{-}PhC{\equiv}CPh)Tp'][BF_4]$,[15] $[Fe(\eta\text{-}C_5H_5)_2][PF_6]$ and $[Fe(\eta\text{-}C_5H_4COMe)(\eta\text{-}C_5H_5)][BF_4]$[25] were prepared by published methods. Thiophenol (Lancaster Chemicals), NaSMe (Acros) and NaSPh (Fluka) were used without further purification.

IR spectra were recorded on a Perkin Elmer Spectrum One FT Spectrometer; NMR spectra were recorded on a JEOL Eclipse 300 spectrometer, operating at 299.9 MHz for ^1H, at 75.4 MHz for ^{13}C, and at 121.4 MHz for ^{31}P, using JEOL Delta software. For ^1H and $^{13}C\text{-}\{^1H\}$ spectra, either $SiMe_4$ or residual protio solvent was used as an internal standard. For $^{31}P\text{-}\{^1H\}$ spectra, 85% H_3PO_4 was used as an external standard. X-band ESR spectra were recorded on a Bruker ESP300E spectrometer equipped with a Bruker variable temperature accessory and a Hewlett-Packard 5350B microwave frequency counter. The field calibration was checked by measuring the resonance of the diphenylpicrylhydrazyl (dpph) radical before each series of spectra.

Electrochemical studies were carried out using an EG&G Model 273A potentiostat linked to a computer using EG&G Model 270 Research Electrochemistry software in conjunction with a three-electrode cell. The auxiliary electrode was a platinum wire and the working electrode a platinum disc (1.6 mm diameter). The reference was an aqueous saturated calomel electrode separated from the test solution by a fine porosity frit and an agar bridge saturated with KCl. Solutions were 1.0×10^{-3} mol dm^{-3} in the test compound and 0.1 mol dm^{-3} in $[NBu^n_4][PF_6]$ as the supporting electrolyte with CH_2Cl_2 as the solvent. Under the conditions used, $E^{o\prime}$ for the one-electron oxidation of $[Fe(\eta\text{-}C_5H_4COMe)(\eta\text{-}C_5H_5)]$, $[Fe(\eta\text{-}C_5H_5)_2]$ and $[Fe(\eta\text{-}C_5Me_5)_2]$, added to the test solutions as internal calibrants, are 0.74, 0.47 and –0.08 V respectively.

Microanalyses were carried out by the staff of the Microanalytical Service of the School of Chemistry, University of Bristol.

Syntheses

$[Mo(SPh)(CO)(\eta\text{-}MeC{\equiv}CMe)(\eta\text{-}C_5H_5)]$ 2. To a stirred suspension of $[Mo(CO)(\eta\text{-}MeC{\equiv}CMe)_2(\eta\text{-}C_5H_5)][BF_4]$ (387 mg, 1.07 mmol) in thf (20 cm^3) was added HSPh (0.11 cm^3, 1.07 mmol) and NEt_3 (0.149 cm^3, 1.07 mmol). The solution, which immediately became brown, was stirred for 30 min and then the mixture was evaporated to dryness *in vacuo*. The residue was extracted with diethyl ether (20 cm^3) and the extract filtered before evaporation to dryness *in vacuo*. The resulting brown residue was dissolved in the minimum volume of CH_2Cl_2 (*ca.* 3 cm^3) and then placed on an alumina–*n*-hexane chromatography column. Elution with *n*-hexane–diethyl ether (1 : 10) gave a red band which was collected and evaporated to dryness *in vacuo*. Crystallisation from *n*-hexane at −78 °C gave red needles of $[Mo(SPh)(CO)(\eta\text{-}MeC{\equiv}CMe)(\eta\text{-}C_5H_5)]$, yield 288 mg (81%).

The complexes $[Mo(SMe)(CO)(\eta\text{-}MeC{\equiv}CMe)(\eta\text{-}C_5H_5)]$ **1**, $[Mo(SMe)(CO)(\eta\text{-}PhC{\equiv}CPh)(\eta\text{-}C_5H_5)]$ **3** and $[Mo(SPh)(CO)(\eta\text{-}PhC{\equiv}CPh)(\eta\text{-}C_5H_5)]$ **4** were prepared similarly. For the SMe complexes, NaSMe was used in place of HSPh and NEt_3.

$[W(SPh)(CO)(\eta\text{-}MeC{\equiv}CMe)(\eta\text{-}C_5H_5)]$ 6. To a stirred suspension of $[W(CO)(\eta\text{-}MeC{\equiv}CMe)_2(\eta\text{-}C_5H_5)][BF_4]$ (100 mg, 0.184 mmol) in thf (30 cm^3) was added HSPh (0.023 cm^3, 0.224 mmol) and NEt_3 (0.031 cm^3, 0.223 mmol). The reaction mixture, which became orange after 30 min, was stirred for 1 h before being evaporated to dryness *in vacuo*. The residue was extracted with diethyl ether (30 cm^3) and the extract filtered and then evaporated to dryness *in vacuo*. The resulting orange residue was dissolved in the minimum volume of CH_2Cl_2 (*ca.* 2 cm^3) and placed on an alumina–*n*-hexane chromatography column. Elution with *n*-hexane–diethyl ether (1 : 1) gave an orange band which was collected and evaporated to dryness *in vacuo*. Crystallisation from diethyl ether at –20 °C gave $[W(SPh)(CO)(\eta\text{-}MeC{\equiv}CMe)(\eta\text{-}C_5H_5)]$ as an orange solid, yield 47 mg (57%).

The compound $[W(SMe)(CO)(\eta\text{-}MeC{\equiv}CMe)(\eta\text{-}C_5H_5)]$ **5** was prepared similarly.

$[Mo(SPh)\{P(OMe)_3\}(\eta\text{-}MeC{\equiv}CMe)(\eta\text{-}C_5H_5)]$ 8. To a stirred suspension of $[Mo\{P(OMe)_3\}_2(\eta\text{-}MeC{\equiv}CMe)(\eta\text{-}C_5H_5)][BF_4]$

(200 mg, 0.364 mmol) in thf (30 cm^3) was added HSPh (0.037 cm^3, 0.364 mmol) and NEt_3 (0.050 cm^3, 0.364 mmol). The solution, which became dark blue after 30 min, was stirred for 1 h and then the mixture was evaporated to dryness *in vacuo.* The residue was extracted with diethyl ether (30 cm^3) and the extract filtered The solvent was then removed and the blue residue dissolved in the minimum volume of CH_2Cl_2 (*ca.* 3 cm^3) and placed on an alumina–*n*-hexane chromatography column. Elution with *n*-hexane–diethyl ether (1 : 4) gave a blue band which was collected and evaporated to dryness *in vacuo*. Crystallisation from *n*-hexane at –78 °C gave blue needles of [Mo(SPh){P(OMe)$_3$}(η-MeC≡CMe)(η-C_5H_5)], yield 117 mg (72%).

The complexes [Mo(SMe){P(OMe)$_3$}(η-MeC≡CMe)(η-C_5H_5)] **7**, [Mo(SMe){P(OMe)$_3$}(η-PhC≡CPh)(η-C_5H_5)] **9** and [Mo(SPh){P(OMe)$_3$}(η-PhC≡CPh)(η-C_5H_5)] **10** were prepared similarly.

[W(SPh){P(OMe)$_3$}(η-MeC≡CMe)(η-C_5H_5)] 11. To a stirred suspension of [W{P(OMe)$_3$}$_2$(η-MeC≡CMe)(η-C_5H_5)][BF_4] (176 mg, 0.256 mmol) in thf (30 cm^3) was added HSPh (0.027 cm^3, 0.253 mmol) and NEt_3 (0.035 cm^3, 0.253 mmol). The reaction mixture, which became pink after 20 min, was stirred for 2 h and then evaporated to dryness *in vacuo*. The pink residue was extracted with diethyl ether (30 cm^3) and the extract filtered. The filtrate was then evaporated to dryness *in vacuo* and the resulting pink residue dissolved in the minimum volume of CH_2Cl_2 (*ca.* 3 cm^3) and placed on an alumina–*n*-hexane chromatography column. Elution with *n*-hexane–diethyl ether (1 : 1) gave a pink solution which was collected and evaporated to dryness *in vacuo*. Crystallisation from diethyl ether at -78 °C gave [W(SPh){P(OMe)$_3$}(η-MeC≡CMe)(η-C_5H_5)] as a pink solid, yield 93 mg (66%).

[W(SMe)(CO)(η-PhC≡CPh)Tp′] 12. To a stirred solution of [W(CO)$_2$(η-PhC≡CPh)Tp′][BF_4] (580 mg, 0.723 mmol) in thf (120 cm^3) was added NaSMe (61 mg, 0.868 mmol). After 3 h, the green solution was evaporated to dryness *in vacuo*. The green residue was redissolved in diethyl ether (50 cm^3) and filtered, silica was added to the solution and then the mixture was dried *in vacuo*. The residue was placed on a silica–*n*-hexane chromatography column. Elution with *n*-hexane–diethyl ether (10 : 1) gave a green band which was collected and evaporated to dryness *in vacuo*. Purification using CH_2Cl_2–*n*-hexane gave the product as a green solid, yield 97 mg (18%).

The complex [W(SPh)(CO)(η-PhC≡CPh)Tp′] **13** was prepared similarly.

[W(SMe)(CO)(η-PhC≡CPh)Tp′][BF_4] 12$^+$[BF_4]$^-$. To a stirred solution of [W(SMe)(CO)(η-PhC≡CPh)Tp′] (84 mg, 0.114 mmol) in CH_2Cl_2 (25 cm^3) was added [Fe(η-C_5H_4COMe)(η-C_5H_5)][BF_4] (35 mg, 0.112 mmol). After 10 min, the green solution was filtered, *n*-hexane (50 cm^3) was added, and the volume of the solution reduced *in vacuo*, inducing precipitation of a dark-green solid which was washed with *n*-hexane (2 × 10 cm^3) and diethyl ether (3 × 10 cm^3), yield 61 mg (65%).

The complex [W(SPh)(CO)(η-PhC≡CPh)Tp′][BF_4] **13**$^+$[BF_4]$^-$ was prepared similarly.

Crystal structure determinations of [Mo(SMe)(CO)(η-MeC≡CMe)(η-C_5H_5)] 1, [Mo(SMe)(CO)(η-PhC≡CPh)(η-C_5H_5)] 3, [Mo(SPh)(CO)(η-PhC≡CPh)(η-C_5H_5)] 4, [Mo(SMe){P(OMe)$_3$}(η-MeC≡CMe)(η-C_5H_5)] 7, [Mo(SPh){P(OMe)$_3$}(η-MeC≡CMe)(η-C_5H_5)] 8, [W(SPh){P(OMe)$_3$}(η-MeC≡CMe)-(η-C_5H_5)] 11, [W(SMe)(CO)(η-PhC≡CPh)Tp′] 12, [W(SPh)(CO)(η-PhC≡CPh)Tp′] 13 and [W(SPh)-(CO)(η-PhC≡CPh)Tp′][PF_6] 13$^+$[PF_6]$^-$

Crystals of [Mo(SMe)(CO)(η-MeC≡CMe)(η-C_5H_5)] **1**, [Mo-(SMe)(CO)(η-PhC≡CPh)(η-C_5H_5)] **3**, [Mo(SPh)(CO)(η-PhC≡CPh)(η-C_5H_5)] **4**, [Mo(SMe){P(OMe)$_3$}(η-MeC≡CMe)(η-C_5H_5)] **7**, [Mo(SPh){P(OMe)$_3$}(η-MeC≡CMe)(η-C_5H_5)] **8**, [W(SPh){P(OMe)$_3$}(η-MeC≡CMe)(η-C_5H_5)] **11**, [W(SMe)(CO)-(η-PhC≡CPh)Tp′] **12**, [W(SPh)(CO)(η-PhC≡CPh)Tp′] **13** and [W(SPh)(CO)(η-PhC≡CPh)Tp′][PF_6] **13**$^+$[PF_6]$^-$ were grown at –20 °C by allowing *n*-hexane to diffuse into a concentrated solution of the complex in CH_2Cl_2.

Many of the details of the structure analyses of **1**, **3**, **4**, **7**, **8**, **11–13** and **13**$^+$[PF_6]$^-$ are listed in Table 5. Diffraction intensities were collected on a Bruker SMART CCD diffractometer, with graphite-monochromated Mo-Kα (0.71073 Å) radiation, and corrected for absorption using *SADABS*.[26] The structures were solved by *SHELXS-97*, expanded by Fourier-difference syntheses, and refined with the *SHELXL-97* package incorporated into the *SHELXTL* crystallographic package.[27] The positions of the hydrogen atoms were calculated by assuming ideal geometries but were not refined. All non-hydrogen atoms were refined with anisotropic thermal parameters by full-matrix least-squares procedures on F^2. The structure of **13** has two crystallographically independent molecules within the asymmetric unit, designated **13A** and **13B** in Table 4. The solution of this structure revealed many small electron-density peaks which could not be satisfactorily modelled, and the data were therefore treated with the PLATON SQUEEZE routine.[28] This calculated that each unit cell contained four voids of 411 $Å^3$, each holding about 90 electrons (which may correspond to two badly disordered dichloromethane molecules).

CCDC reference numbers 738814–738822. For crystallographic data in CIF or other electronic format see DOI: 10.1039/b912986c

Acknowledgements

We thank the University of Bristol (E.P.), the EPSRC (A.B.) and the Royal Thai Government (S.B. and A.K.) for Postgraduate Scholarships.

References

1 C. J. Adams, I. M. Bartlett, S. Boonyuen, N. G. Connelly, D. J. Harding, O. D. Hayward, E. J. L. McInnes, A. G. Orpen, M. J. Quayle and P. H. Rieger, *Dalton Trans.*, 2006, 3466.
2 C. J. Adams, I. M. Bartlett, S. Carlton, N. G. Connelly, D. J. Harding, O. D. Hayward, A. G. Orpen, E. Patrón, C. D. Ray and P. H. Rieger, *Dalton Trans.*, 2007, 62.
3 C. J. Adams, K. M. Anderson, N. G. Connelly, D. J. Harding, O. D. Hayward, A. G. Orpen, E. Patrón and P. H. Rieger, *Dalton Trans.*, 2009, 530.
4 P. S. Braterman, J. L. Davidson and D. W. A. Sharp, *J. Chem. Soc., Dalton Trans.*, 1976, 241.
5 J. A. K. Howard, R. F. D. Stansfield and P. Woodward, *J. Chem. Soc., Dalton Trans.*, 1976, 246.

6 J. L. Davidson, M. Green, F. G. A. Stone and A. J. Welch, *J. Chem. Soc., Dalton Trans.*, 1977, 287.
7 J. L. Davidson, *J. Chem. Soc., Dalton Trans.*, 1986, 2423.
8 J. L. Davidson and F. Sence, *J. Organomet. Chem.*, 1991, **409**, 219.
9 S. R. Allen, T. H. Glauert, M. Green, K. A. Mead, N. C. Norman, A. G. Orpen, C. J. Schaverien and P. Woodward, *J. Chem. Soc., Dalton Trans.*, 1984, 2747.
10 C. C. Philipp, C. G. Young, P. S. White and J. L. Templeton, *Inorg. Chem.*, 1993, **32**, 5437.
11 J. L. Caldarelli, P. S. White and J. L. Templeton, *J. Am. Chem. Soc.*, 1992, **114**, 10097.
12 S. Boonyuen, PhD thesis, University of Bristol, 2005.
13 J. L. Davidson, M. Green, F. G. A. Stone and A. J. Welch, *J. Chem. Soc., Dalton Trans.*, 1976, 738; C. Carfagna, M. Green, K. R. Nagle, D. J. Williams and C. M. Woolhouse, *J. Chem. Soc., Dalton Trans.*, 1993, 1761.
14 D. M. Tellers, S. J. Skoog, R. G. Bergman, T. B. Gunnoe and W. D. Harman, *Organometallics*, 2000, **19**, 2428.
15 S. G. Feng, C. C. Philipp, A. S. Gamble, P. S. White and J. L. Templeton, *Organometallics*, 1991, **10**, 3504.
16 J. L. Templeton, *Adv. Organomet. Chem.*, 1989, **29**, 1.
17 H. G. Alt, *J. Organomet. Chem.*, 1985, **288**, 149.
18 B. E. R. Schilling, R. Hoffmann and J. W. Faller, *J. Am. Chem. Soc.*, 1979, **101**, 592.
19 J. L. Templeton, P. B. Winston and B. C. Ward, *J. Am. Chem. Soc.*, 1981, **103**, 7713.
20 R. M. Silverstein and F. X. Webster, *Spectrometric Identification of Organic Compounds*, John Wiley & Sons Inc., New York, 1998, 6th ed., p. 154.
21 M. Herberhold, H. G. Alt and C. G. Kreiter, *J. Organomet. Chem.*, 1972, **42**, 413.
22 A. G. Orpen, L. Brammer, F. H. Allen, O. Kennard, D. G. Watson and R. Taylor, *J. Chem. Soc., Dalton Trans.*, 1989, S1.
23 M Bottrill and M. Green, *J. Chem. Soc., Dalton Trans.*, 1977, 2365 .
24 P. L. Watson and R. G. Bergman, *J. Am. Chem. Soc.*, 1980, **102**, 2698.
25 N. G. Connelly and W. E. Geiger, *Chem. Rev.*, 1996, **96**, 877.
26 G. M. Sheldrick, *SADABS*, Version 2.03 (2003), University of Göttingen, Germany.
27 G. M. Sheldrick, *Acta Crystallogr., Sect. A: Found. Crystallogr.*, 2008, **64**, 112.
28 A. L. Spek, *Acta Crystallogr., Sect. A: Found. Crystallogr.*, 1990, **46**, C34; A. L. Spek, *PLATON–A Multipurpose Crystallographic Tool*, Utrecht University, Utrecht, The Netherlands, 2006.

